# High-dynamic baseline determination for the Swarm constellation

Mao, X.; Visser, P. N.A.M.; van den IJssel, J.

**DOI**
10.1016/j.ast.2019.03.031

**Publication date**
2019

**Document Version**
Accepted author manuscript

**Published in**
Aerospace Science and Technology

# High-dynamic baseline determination for the Swarm constellation

X. Mao[a,*], P.N.A.M. Visser[a], J. van den IJssel[a]

[a] *Delft University of Technology, Kluyverweg 1, 2629 HS Delft, The Netherlands*

**Abstract**

Baseline determination for the European Space Agency Swarm magnetic field mission is investigated. Swarm consists of three identical satellites -A, -B and -C. The Swarm-A and -C form a pendulum formation whose baseline length varies between about 30 and 180 km. Swarm-B flies in a higher orbit, causing its orbital plane to slowly rotate with respect to those of Swarm-A and -C. This special geometry results in short periods when the Swarm-B satellite is adjacent to the other Swarm satellites. Ten 24-hr periods around such close encounters have been selected, with baseline lengths varying between 50 and 3500 km. All Swarm satellites carry high-quality, dual-frequency and identical Global Positioning System receivers not only allowing precise orbit determination of the single Swarm satellites, but also allowing a rigorous assessment of the capability of precise baseline determination between the three satellites. These baselines include the high-dynamic baselines between Swarm-B and the other two Swarm satellites.

For all orbit determinations, use was made of an Iterative Extended Kalman Filter approach, which could run in single-, dual-, and triple-satellite mode. Results showed that resolving the issue of half-cycle carrier phase ambiguities (present in original release of GPS RINEX data) and reducing the code observation noise by the German Space Operations Center converter improved the consistency of reduced-dynamic and kinematic baseline solutions for both the

*Corresponding author; Tel.:+31 (0)15 27 82065; Fax:+31(0)15 27 82072
*Email address:* x.mao@tudelft.nl (X. Mao)

Swarm-A/C pendulum pair and other combinations of Swarm satellites. All modes led to comparable consistencies between the computed orbit solutions and satellite laser ranging observations at a level of 2 cm. In addition, the consistencies with single-satellite ambiguity fixed orbit solutions by the German Space Operations Center are at comparable levels for all the modes, with reduced-dynamic baseline consistency at a level of 1-3 mm for the pendulum Swarm-A/C formation and 3-5 mm for the high-dynamic Swarm-B/A and -B/C satellite pairs in different directions.

*Keywords:* Precise Baseline Determination, Precise Orbit Determination, Swarm, Ambiguity fixing, Half-cycle ambiguity

---

## 1. Introduction

Satellite formations and constellations have been increasingly utilized to fulfill various research objectives [1]. Data collected by their on-board instruments offer adequate information to satisfy complex scientific and operational tasks. For instance, two Low Earth Orbiting (LEO) satellites in close formation are used for observing the temporal and spatial variations of Earth's gravity field [2] or for producing digital elevation maps [3]. As a prerequisite for these state-of-the-art applications, satellite orbits and especially also baselines have to be precisely determined, the latter with (sub-)mm level precision. Precise baseline solutions are crucial for *e.g.* interferometric Synthetic Aperture Radar (SAR) missions [4] and have the potential benefit of supporting gravity field research [5].

Formation flying LEO satellites typically make use of high precision, dual-frequency multi-channel GPS receivers for Precise Orbit Determination (POD) [6]. By forming Double-Differenced (DD) carrier phase observations, common errors are strongly mitigated and so-called integer ambiguities can be resolved [7]. With the advent of the GRACE mission [2], it has been proved that Precise Baseline Determination (PBD) at 1-mm level is feasible by fixing DD carrier phase ambiguities [8]. Further improvements are obtained by making use of

relative dynamics constraints and GPS receiver antenna patterns. Nowadays, sub mm level baseline precision is achievable for in-line or along-track formations like the Gravity Recovery and Climate Experiment (GRACE) mission [9, 10, 11]. For a more complex side-by-side or radial/cross-track formation such as the TanDEM-X/TerraSAR-X mission, it is claimed that a precision in each direction of 3-8 mm can be achieved [4]. On 22 November 2013, the European Space Agency (ESA) geomagnetic field mission Swarm was launched and soon the three Swarm satellites entered their preferred orbits by a series of dedicated maneuvers [12]. It is an unprecedented three-identical-satellite constellation equipped with the same space-borne instruments. All Swarm satellites fly in near-polar orbits, with Swarm-A/C in a pendulum formation and Swarm-B at a higher altitude [12]. The distance between the Swarm-A and -C satellites is varying between 30 and 180 km. When Swarm-B is in view of the other Swarm satellites, the distance can be as small as about 50 km. For the pendulum part of Swarm, PBD has already been studied in detail, showing that consistencies between reduced-dynamic and kinematic solutions under different in-flight environment can be achieved that are of the order of 5-40 mm in different directions [13, 14]. At present, no successful consistently high-precision high-dynamic PBD research has been done for such kind of constellation.

Obtaining very precise baseline solutions for LEO satellites that do not fly in stable formation is still an open issue. For example, the work described in [15] shows that it is not straightforward to achieve precise baseline solutions between the CHAMP and GRACE satellites when these satellites are in view of each other. The CHAMP-GRACE baselines grow easily from hundreds of kms to thousands of kms in one day and these are therefore referred to as high-dynamic baselines. The same applies to the Swarm-B satellite with respect to the Swarm-A and -C satellites. As the baseline - or distance - between two LEO satellites grows, the number of GPS satellites that are simultaneously in view of two GPS receivers drops, resulting in a smaller number of possible DD combinations. Moreover, LEO satellites experience different perturbing forces when at different altitudes, especially atmospheric drag due to different density

levels [16].

The three-identical-satellite Swarm constellation will be used as a test bed for high dynamic baseline determination between LEO satellites. The results in [15] are based on 24-hr orbital arcs that start and end at midnight, which leads to significantly different CHAMP-GRACE orbital geometries for each arc. Moreover, CHAMP and GRACE carry GPS BlackJack receivers with different performance and also have different antenna installation geometries [17]. For CHAMP and occasionally for GRACE, also so-called cross-talk signal interference between the POD and radio occultation antenna's took place leading to different multi-path patterns [18, 11]. For Swarm, this is not the case. Compared to the work described in [15], a different approach is adopted for defining the orbital arcs. A total of 10 days are identified in the period from mid-July to mid-September in 2014 when the Swarm satellites are frequently in view of each other. The time of closest approach is then determined and a 24-hr orbital arc is defined starting 12 hr before and ending 12 hr after this time. This leads to comparable and more stable geometries for each selected orbital arc.

The *RUAG Space* Swarm GPS receiver exhibits half- and full-cycle ambiguities due to the tracking issue with its Numerically Controlled Oscillator (NCO) [19, 14]. Systematic 180° phase rotation frequently happens during the tracking process [20]. This makes carrier phase integer ambiguity fixing more challenging. Fixing half-cycle ambiguities erroneously to full-cycle will significantly downgrade the baseline solution precision for the lower pair [10]. This receiver characteristic has thus to be properly dealt with. The German Space Operations Center (GSOC/DLR) has implemented an algorithm to correct the half-cycles into full-cycles by checking a certain bit of each carrier phase tracking record in the raw data [20]. In addition, a systematic GPS RINEX converter software issue existed for code observations, leading to larger code noise at the early stage of the Swarm mission and was fixed by ESA on 11 April 2016 (https://earth.esa.int/web/guest/missions/esa-operational-eo-missions/swarm/news/-/article/swarm-software-issue-in-rinex-converter-fixed, last accessed: 9 January 2019). ESA has been re-creating

these old Swarm RINEX files with both issues removed (the 8th Swarm Data Quality Workshop, https://earth.esa.int/web/guest/missions/esa-eo-missions/swarm/activities/conferences/8th-data-quality-workshop, last accessed: 9 January 2019). The resulting GPS data lead to significantly more precise single-satellite POD [21] and dual-satellite PBD solutions for the Swarm-A/C formation [14, 13]. Their impacts on the high-low satellite pairs will be investigated in this research.

For the Swarm mission, it is not possible to validate PBD solutions by comparison with independent data coming from for example a K-band Radar Ranging system as on board the GRACE twin satellites [22]. A quality check can typically be done by assessing the consistency between kinematic and reduced-dynamic baseline solutions [5, 10, 13]. Moreover, external POD and PBD solutions are available and can be used for a quality assessment. An interesting development is single receiver ambiguity fixing, leading to enhanced POD solutions [23, 20]. [23] propose a scheme of ambiguity fixing based on the ionosphere-free wide-lane model developed by [24], while [20] make use of the wide-lane phase bias estimate products provided by [25]. Such single-satellite ambiguity fixed POD solutions have been made kindly available by GSOC/DLR for Swarm and will be used for assessing the quality of both POD and PBD orbit solutions in this research [21]. Details of the single-satellite ambiguity fixed POD solutions can be found in [20] for the Sentinel-3A satellite, which carries a GPS receiver with similar characteristics when comparing with those flown by Swarm. An external validation of the individual satellite orbit solutions is offered by the availability of Satellite Laser Ranging (SLR) observations, which will form part of the analysis and quality assessments [26].

The structure of this paper is as follows. Section 2 includes a description of the Swarm constellation data selection and corresponding quality assessment. Section 3 introduces the kinematic and reduced-dynamic POD and PBD algorithms. Section 4 describes results and orbit comparisons for the Swarm constellation. This paper is concluded by Section 5, which includes a summary and outlook.

## 2. Observations

### *2.1. Data selection*

Representative data have been selected to test PBD for all three Swarm satellites. Table 1 includes three selected Keplerian orbital elements for Swarm satellites at a representative epoch. The Swarm-A/C formation flies in two almost identical polar orbits with only 1.5° difference in the right ascension of the ascending node (RAAN). These two satellites form a so-called pendulum formation. During the analyzed period the Swarm-B satellite flies about 50 km higher, which slightly differs with the early designed orbit scheme [12, 27], and the RAAN difference on average is about 10°. Baseline lengths of high-low Swarm satellite pairs thus vary dramatically due to the different orbital planes and altitudes. It is found that the period July-September 2014 includes days for which the Swarm-A/B/C geometry is favorable, *i.e.* all three satellites are in view of each other. During this period, the baseline lengths between the Swarm-B satellite on the one hand and the Swarm-A and -C satellites on the other hand reach a local minimum every 6.1 days.

To evaluate the PBD methods used in this research, a sliding 24-hr orbit arc selection is done. Each selected orbit arc centers around the epoch of minimum distance, see *e.g.* Figure 1. The Swarm-A/C formation baseline length varies consistently between 30 and 180 km. For the Swarm-B/A and Swarm-B/C pairs, the two satellites approach each other from an approximate 3500 km to a minimum of around 50 km. Ten orbit arcs are selected and recorded in Table 2. The used GPS ephemeris products are separate 24-hr GPS satellite orbits and 5-sec clock biases files [28]. Before making use of them, a tool is used to interpolate the adjacent three consecutive 24-hr GPS satellite orbits into 5 seconds and then a merged orbit and clock file is created. The influence of GPS orbit and clock bias gaps crossing midnight is reduced.

Figure 2 shows that the Swarm-A/C pendulum formation has on average $> 7$ common GPS satellites in view. This number is not yet influenced by the antenna field of view modification and is approximately equal to the number of

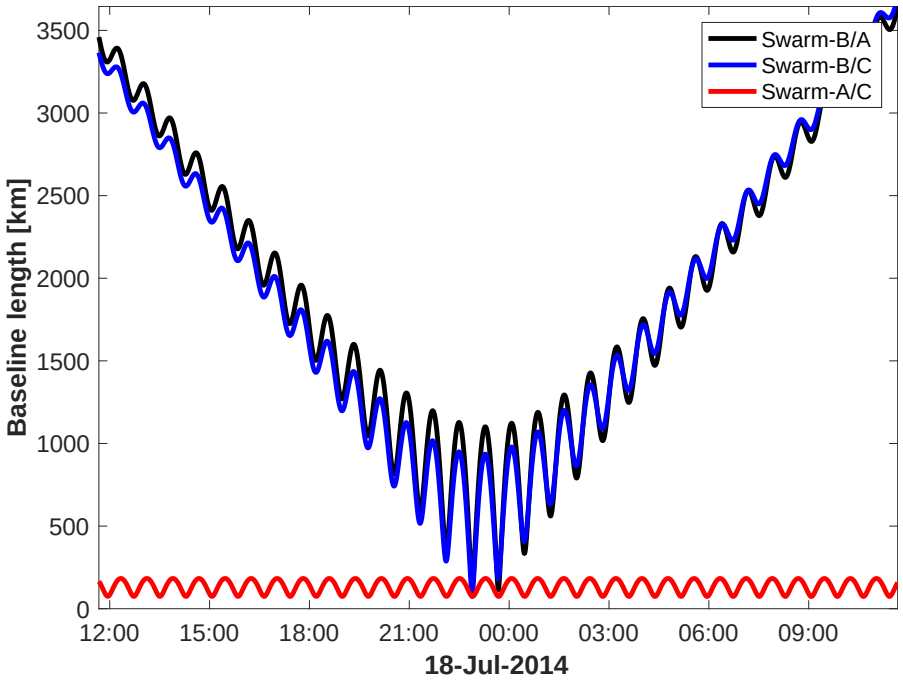


Figure 1: Length variations for each Swarm dual-satellite formation during one representative 24-hr orbit arc.

Table 1: The crucial Keplerian orbital elements determining the relation between Swarm orbital planes during mid-July to mid-September 2014. $a$ represents the semi-major axis, $i$ means the orbit inclination and $\Omega$ is the right ascension of the ascending node (Credit: satellite two line elements data is obtained from www.space-track.org).

| Satellite | $a$ (km) | $i$ (deg) | $\Omega$ (deg) |
|---|---|---|---|
| Swarm-A | 6842.06-6840.75 | 87.35-87.36 | 197.53-175.66 |
| Swarm-C | 6842.05-6840.75 | 87.35-87.36 | 198.70-177.03 |
| Swarm-B | 6890.98-6890.41 | 87.75-87.76 | 206.28-188.59 |

Table 2: Ten selected 24-hr orbit arcs for Swarm constellation. Please note that DOY specifies the day of the center of the arc. This DOY number will be used as orbit arc identifier in this research.

| Date (YYYY-MM-DD) | DOY | Middle of the arc | Minimum distance (km) |
|---|---|---|---|
| 2014-07-17 | 198 | 23:40:30 | 112.57 |
| 2014-07-24 | 205 | 02:50:40 | 85.69 |
| 2014-07-30 | 211 | 06:00:40 | 82.85 |
| 2014-08-05 | 217 | 08:23:30 | 120.39 |
| 2014-08-11 | 223 | 11:33:00 | 56.14 |
| 2014-08-17 | 229 | 13:55:10 | 51.84 |
| 2014-08-23 | 235 | 16:17:20 | 52.51 |
| 2014-08-29 | 241 | 18:39:10 | 70.62 |
| 2014-09-04 | 247 | 20:13:40 | 58.99 |
| 2014-09-10 | 253 | 21:47:50 | 64.91 |

GPS receiver tracking channels [13]. For the high-low Swarm satellite pairs, this number drops from 6-8 to 4-6 as the baselines become longer. A low number of common GPS satellites in view has a big impact on the achievable PBD precision, especially for kinematic solutions. For high-quality PBD, at least 5 GPS satellites are required to be simultaneously tracked by two GPS receivers [8]. If less than 5 GPS satellites are commonly in view, no kinematic PBD solution will be generated for the associated epochs. Reduced-dynamic baseline

solutions will then however still be available.

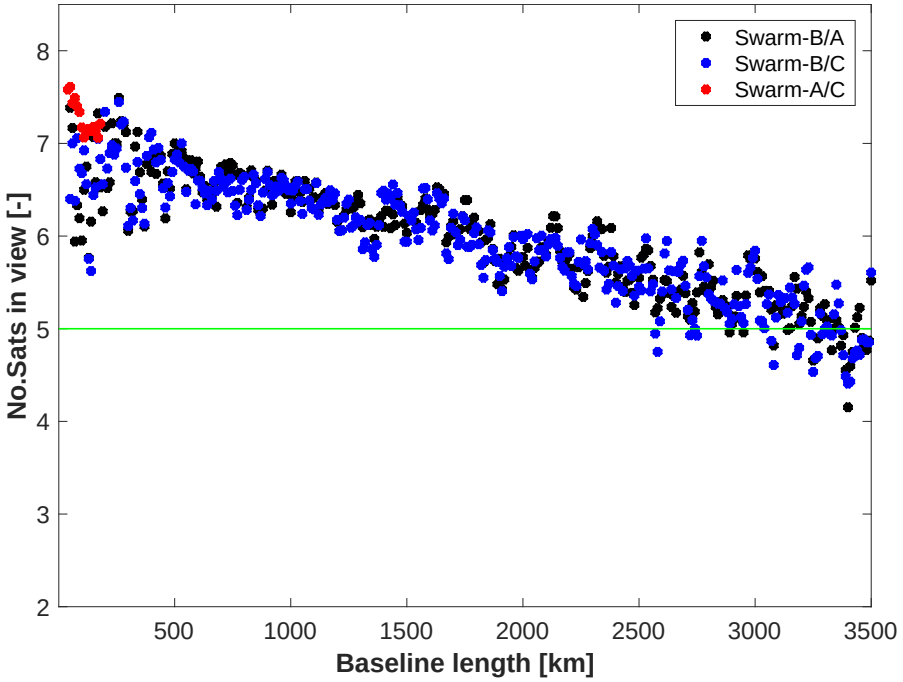


Figure 2: The number of GPS satellites simultaneously tracked by two GPS receivers as a function of distance (every 10 kms) for each Swarm dual-satellite formation (analysis for 10 24-hr orbit arcs).

### *2.2. Data quality assessment*

GPS code and carrier phase observations are affected by several error sources, including thermal noise and multi-path. For the relevant Swarm data used in this research, the original GPS code observations suffer additionally from systematic errors due to sub optimal RINEX converter software leading to large noise levels. The code noise level has a clear impact on the ambiguity fixing success rate. The original carrier phase observations experience half-cycle ambiguity issues as mentioned above. A new version of Swarm GPS data was kindly provided by GSOC/DLR. For this version, the converter code error was removed and in addition the half-cycle carrier phase ambiguities were corrected to full-cycles.

The quality of in-flight GPS code observations can be assessed by analyzing their multi-path effects by using the multi-path evaluation models that are introduced in [18, 29]. Thus, the multi-path represents an independent evaluation of misfit caused by the systematic errors from the RINEX converter on the one hand and the code observation noise on the other hand. The Root-Mean-Square (RMS) of multi-path is displayed in Figure 3 for Swarm-A as a function of the elevation of the GPS satellites as seen from the GPS receiver antenna installed on the zenith surface of each Swarm satellite. The results displayed in Figure 3 hold for 17 July 2014, when the Swarm-A GPS antenna had an antenna field of view of 80° (improved to 88° in October, 2014, [30]). The tracked GPS observations below 10° antenna cut-off angle are obtained by the tracking performance of GPS receiver antenna in its aft direction, as reported by [30].

In general, the observation residual level drops with increasing elevation angle, which is in agreement with anticipated noise levels of GPS observations [18]. Modifications in the new version of data clearly reduce the code noise level. This analysis indicates a reduction from 0.34/0.37 m to 0.18/0.20 m in terms of global RMS for the $L_1/L_2$ frequencies. Code noise on the $L_1$ frequency is slightly smaller than on the $L_2$ frequency. It is anticipated that the ambiguity fixing will improve when using the new batch of data.

Research in [14, 13] confirms that the GPS observation correction process implemented by GSOC/DLR has a clear impact on the ambiguity fixing process, as also shown in Figure 4 in this research. This figure is representative for a triple-satellite PBD (see Section 3.1) and displays the ambiguity fixing success rate as a function of the number of iterations completed by the IEKF (with a maximum of 20). In the IEKF procedure, the ambiguities for the pendulum formation Swarm-A/C pair are fixed first (requiring around 6 iterations until convergence), after which as many as possible ambiguities are fixed for the Swarm-B/A and Swarm-B/C pairs. It can be observed that the ambiguity fixing is clearly enhanced by using the new version of the data. For the Swarm-A/C formation, the success rate for the first iteration is improved from 37% to 97%. The final fixing success rate increases from 88% to 98%. For the Swarm-B/A

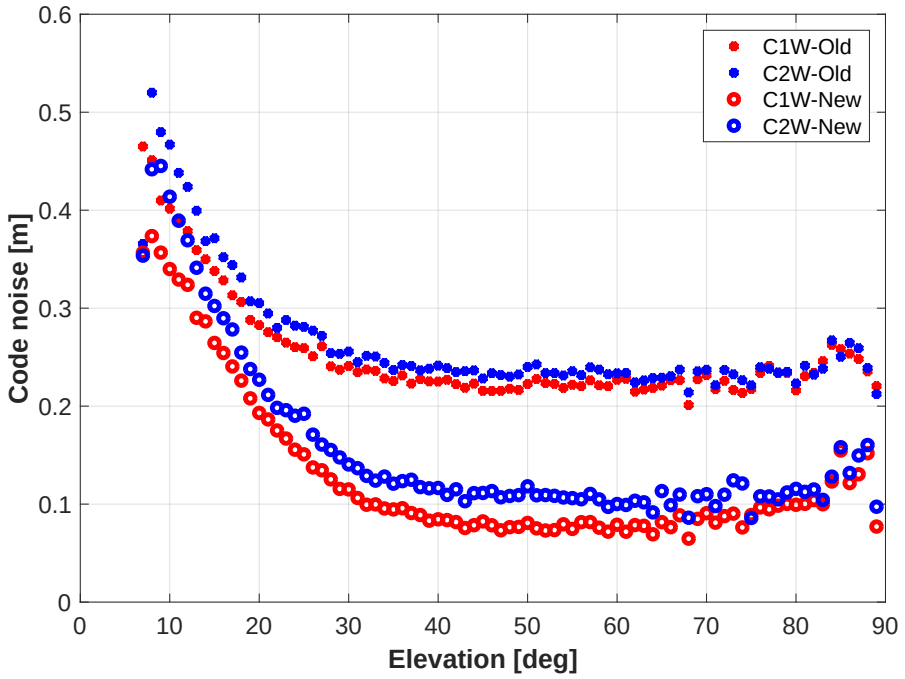


Figure 3: RMS of code multi-path as a function of elevation for the GPS $L_1$ and $L_2$ frequencies for two versions of Swarm-A GPS receiver RINEX data: *Old* indicates the ESA original file with RINEX converter software issues, *New* indicates the one corrected by GSOC/DLR and used in this research (selected day: DOY 198, 2014).

and Swarm-B/C combinations, fixing starts at iteration 8 for the old version of the data and iteration 7 for the new version of the data. It can also be clearly seen that for the starting iteration, the success rate improves from merely 9% and 8% to a much higher level of 64% and 64% for the Swarm-B/A and Swarm-B/C combinations, respectively. The final success rates reach about 97% and 97%, respectively, which is much higher than 81% and 83% when using the old version of the data.

Swarm dual-satellite PBD (again, please see Section 3.1) is done to evaluate the influence of half-cycle *vs.* full-cycle inter ambiguity fixing. As shown in table 3, the ambiguity fixing success rate is improved by more than 10% when full-cycle ambiguities are to be fixed. The new version of the data also im-

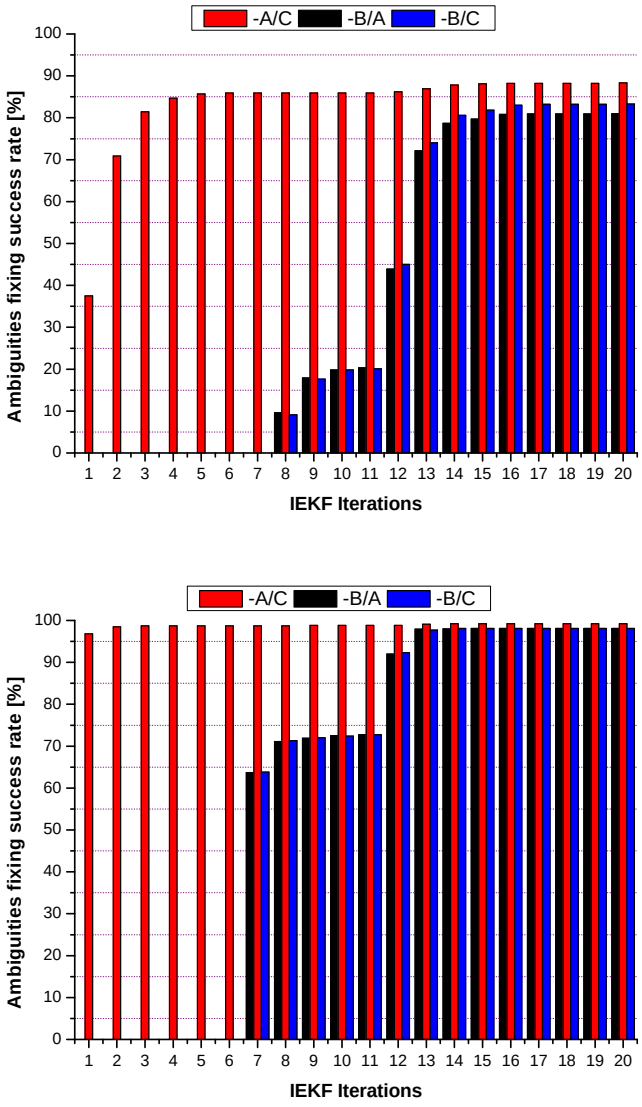


Figure 4: Integer ambiguity fixing success rate versus IEKF iterations for the triple-satellite Swarm PBD. Two sets of data, original version (top) and new version with corrections (bottom) are used (selected day: DOY 198, 2014).

proves the kinematic and reduced-dynamic baseline consistency, especially for two high-dynamic Swarm-B/A and Swarm-B/C satellite pairs. Therefore, for

the remainder of this paper, results will be based on the new version of the data (Section 4).

Table 3: Mean of daily RMS differences between kinematic and reduced-dynamic baseline solutions, and ambiguity fixing success rate for Swarm constellation (dual-satellite PBD solutions). Two sets of Swarm GPS RINEX data are used.

| Solution | Radial (mm) | Along-track (mm) | Cross-track (mm) | Amb.fix. (%) |
|---|---|---|---|---|
| | | **Swarm-A/C** | | |
| Half-cycle | 15.0 | 7.8 | 4.1 | 86.9 |
| Full-cycle | 12.4 | 5.5 | 3.6 | 98.1 |
| | | **Swarm-B/A** | | |
| Half-cycle | 24.9 | 11.2 | 5.3 | 84.2 |
| Full-cycle | 22.9 | 9.8 | 5.6 | 97.3 |
| | | **Swarm-B/C** | | |
| Half-cycle | 24.9 | 11.4 | 6.5 | 83.9 |
| Full-cycle | 22.6 | 10.4 | 5.7 | 97.5 |

## 3. Methodology

### *3.1. Single-, dual- and triple- POD/PBD*

When solely using dual-frequency high-precision GPS tracking data and GPS satellite orbit/clock products, instantaneous satellite positions can be determined at the observation epochs when a sufficient number of GPS satellites is in view. This approach is referred to as kinematic approach [31] and obviously leads to gaps in the position time series when there are gaps in the GPS observation data or when not enough GPS satellites are in view. Dynamic and reduced-dynamic orbit determination, which include force models to solve equations of motion, result in continuous time series of satellite positions [6]. Force

models are typically divided in (1) gravitational force models including the non-spherical gravity field, perturbations from $3^{rd}$ bodies (Sun and the Moon), and solid-earth and ocean tides, and (2) non-gravitational force models including the Sun radiation pressure, the Earth albedo pressure, and atmospheric drag. However, the associated models are not perfect, and model errors can be absorbed by so-called empirical accelerations [17].

The Multiple Orbit Determination using Kalman filtering (MODK, [15]) tool is an in-house developed add-on tool to the GPS High Precision Orbit Determination Software Tools (GHOST) [32]. MODK has the capability to provide reduced-dynamic single-, dual- and triple-satellite orbit solutions, where for the dual- and triple-satellite mode ambiguity fixing as well as further kinematic baseline determination can be done. The core of the MODK tool is based on an Iterative Extended Kalman Filter (IEKF) process, where the GPS observations are used and modeled for each frequency, *i.e.* $L_1$ and $L_2$ [11]. A comprehensive description of the MODK tool and underlying method can be found in Chapter 3.3 of [15].

Compared to single-satellite POD, PBD in case of dual- and triple-satellite orbit determination includes the possibility to constrain differential empirical accelerations, which is especially relevant if two satellites fly in almost identical orbits (as is the case for Swarm-A and -C). This constraining proved to be very beneficial for estimating high-precision baselines for the GRACE tandem and for the Swarm-A/C pendulum formations [10, 13]. In this study the frequency-dependent antenna Phase Center Variation (PCV) maps created by so-called *residual approach* are included [33, 11]. Our proposed Code Residual Variation (CRV) maps are not modelled since the used GSOC/DLR processed data have lower noise levels than the original data. Besides, no significant signal interference exists for Swarm when comparing with GRACE as described in [11].

The MODK tool first computes reduced-dynamic orbit solutions, after which kinematic solutions are generated. The latter are based on the same modeled GPS observations, where use is made of the ambiguity fixing of the reduced-

dynamic solution. In order to minimize gaps in the kinematic satellite position time series, all available fixed integer ambiguities and otherwise float ambiguities are used. No kinematic solutions are computed for epochs for which less than 5 GPS satellites are simultaneously in view of each combination of two GPS receivers, or epochs for which the RMS of GPS observation phase residuals is above 5 cm. A Least Squares Method (LSM) is adopted for the kinematic PBD. More detailed information and the data flow chart regarding the kinematic and reduced-dynamic approaches can be found in [13]. The MODK tool includes the option to define a preferred baseline, *i.e.* a pair of satellites for which the ambiguity fixing is done first, after which the fixing is invoked for the other baselines. For the Swarm triple-satellite PBD, this option is used and the preferred baseline is the one for the pendulum Swarm-A/C satellite pair.

The DD ambiguities are resolved by the Least-squares Ambiguity De-correlation Adjustment (LAMBDA) algorithm [7]. It has been widely used for different satellite formations PBD [8, 10, 11]. To maximize the ambiguity fixing success rate, a subset fixing process is implemented. It allows for part of a set of integer ambiguities to be fixed while for the remaining the associated float values are used. This is not a conventional use of the LAMBDA algorithm, which nominally only accepts epochs when the entire set of ambiguities is fixed [8]. A strict ambiguity fixing validation scheme is adopted and integrated in the MODK tool [34, 11]. Moreover, an additional outlier detection check is included: if the absolute value of GPS carrier phase observation residuals (after fixing) is above 5 cm, the associated ambiguity will be kept at its float value and sent into IEKF for further fixing in the next iterations. It was found that this resulted in a reduced chance of wrongly fixed integer ambiguities and thus a more robust PBD by the IEKF as used by the MODK tool.

### *3.2. Parameter settings*

Due to the different orbit altitudes for the Swarm satellites (Table 1), especially uncertainties in the modeling of non-gravitational accelerations can be different for Swarm-A and -C on the one hand and Swarm-B on the other hand.

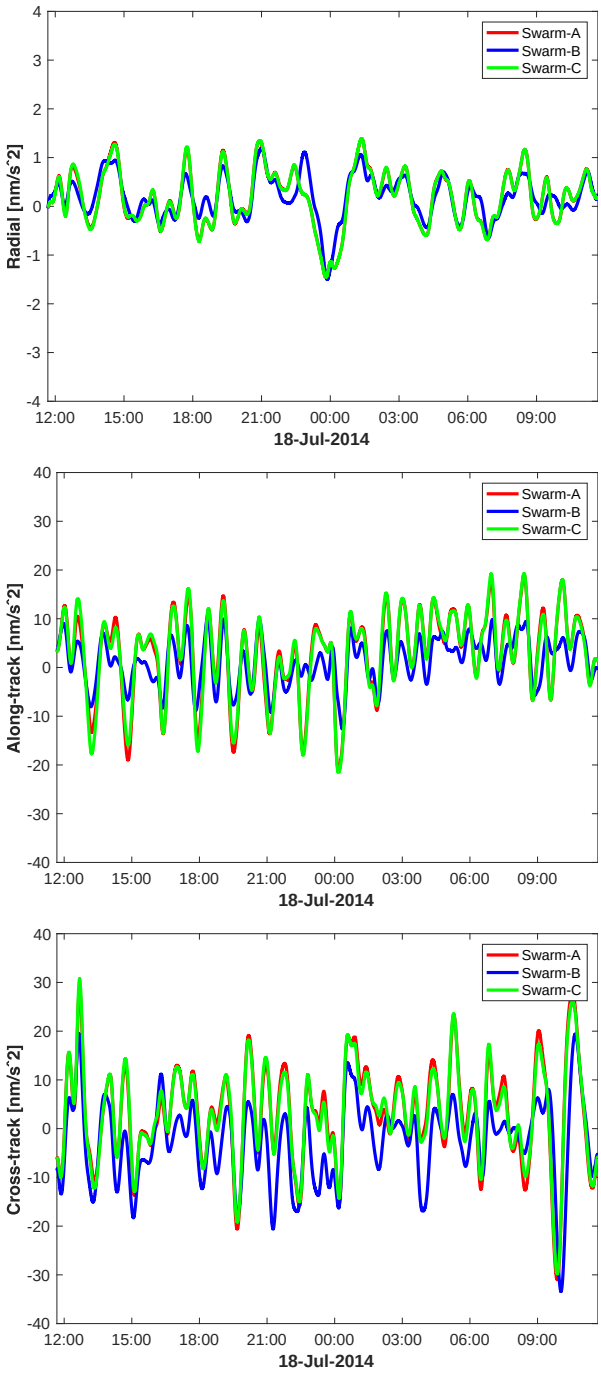


Figure 5: Time series of estimated empirical accelerations in the radial (top), along-track (middle) and cross-track (bottom) directions for each Swarm satellite based on triple-satellite PBD. Please note different scales are set for the vertical axes (DOY 198, 2014). Please note that the curves for Swarm-A and -C almost completely overlap.

This will lead to differences in the estimated empirical accelerations that are used to absorb modeling errors. Figure 5 shows typical levels of estimated empirical accelerations for the three Swarm satellites on a representative day. The statistics of them are shown in Table 4. The mean of estimates of empirical accelerations represents the level of constant correction to the adopted dynamic models in certain direction. Although for all three Swarm satellites, the values seems to overlap to quite a significant extent, the empirical acceleration differences for the Swarm-A/C pair are significantly smaller than for the other pairs. It can be observed that the empirical accelerations (mean and RMS-about-mean) are larger in the along-track direction, which is the direction for which atmospheric drag is predominant, and the cross-track direction, which is the direction for which mis-modeling of solar radiation pressure forces is the largest (also due to the simplified canon ball satellite model that is used by the MODK tool, the scaling factors of the associated non-gravitational forces can not compensate the in-flight perturbations completely [13, 35]).

Table 4: Empirical acceleration estimate statistics for each Swarm satellite and satellite pair (mean and RMS-about-mean, DOY 198, 2014).

| Sat/Pair | Radial ($nm/s^2$) | Along-track ($nm/s^2$) | Cross-track ($nm/s^2$) |
|---|---|---|---|
| Swarm-A | $0.2 \pm 0.6$ | $2.9 \pm 8.2$ | $3.2 \pm 9.8$ |
| Swarm-B | $0.2 \pm 0.4$ | $1.2 \pm 4.6$ | $-2.6 \pm 8.2$ |
| Swarm-C | $0.2 \pm 0.6$ | $3.0 \pm 8.3$ | $3.2 \pm 9.5$ |
| Swarm-A/C | $0.0 \pm 0.0$ | $-0.0 \pm 1.1$ | $-0.0 \pm 1.2$ |
| Swarm-B/A | $0.0 \pm 0.3$ | $-1.7 \pm 5.3$ | $-5.8 \pm 6.5$ |
| Swarm-B/C | $0.0 \pm 0.3$ | $-1.7 \pm 5.4$ | $-5.8 \pm 5.9$ |

The correlation time ($\tau$), STandard Deviation (STD) of a-priori values ($\sigma_a$) and process noise ($\sigma_p$) of empirical accelerations have been tuned to reflect the typical level for these parameters, both in an absolute and relative sense. The adopted values are included in Table 5. It can be seen that the values for the

STD for the difference between empirical accelerations is specified to be smaller for the Swarm-A/C pendulum satellite pair, reflecting their similarity of orbit (especially altitude).

Both GPS carrier phase and code observations are used by MODK to produce orbit solutions. The carrier phase weight is set inversely proportional to its claimed noise level, which is 3 mm for each frequency in POD and 5 mm in PBD as in that case single-differences are used. The code observation weight is set as 0.3 m for each frequency in POD and 0.5 m in PBD. The same force models and standards are used as specified in [13].

Table 5: Empirical acceleration parameter settings in three directions (radial/along-track/cross-track) for each Swarm satellite and each pair of satellites in IEKF. The correlation time $\tau$ is equal to 600 s.

| Sat/Pair | $\sigma_a$ $(nm/s^2)$ | $\sigma_p$ $(nm/s^2)$ |
|---|---|---|
| Swarm-A | 5/15/15 | 1/3/3 |
| Swarm-B | 5/15/15 | 1/3/3 |
| Swarm-C | 5/15/15 | 1/3/3 |
| Swarm-A/C | 2/5/5 | 0.2/1/1 |
| Swarm-B/A | 5/15/15 | 1/3/3 |
| Swarm-B/C | 5/15/15 | 1/3/3 |

## 4. Results and discussion

This section includes the results of the Swarm precise orbit and baseline determination for the selected 10 orbit arcs. The single-satellite ambiguity fixed GSOC/DLR kinematic and reduced-dynamic POD solutions serve as reference both for the absolute and baseline solutions, where the latter is referred to as the GSOC/DLR Differential POD or DPOD solution. Results for both dual-satellite (Section 4.2) and triple-satellite (Section 4.3) PBD will be provided

and discussed, followed by SLR validation (Section 4.4). However, this section starts with a brief result regarding the detection of GPS observation outliers.

### *4.1. GPS data outliers*

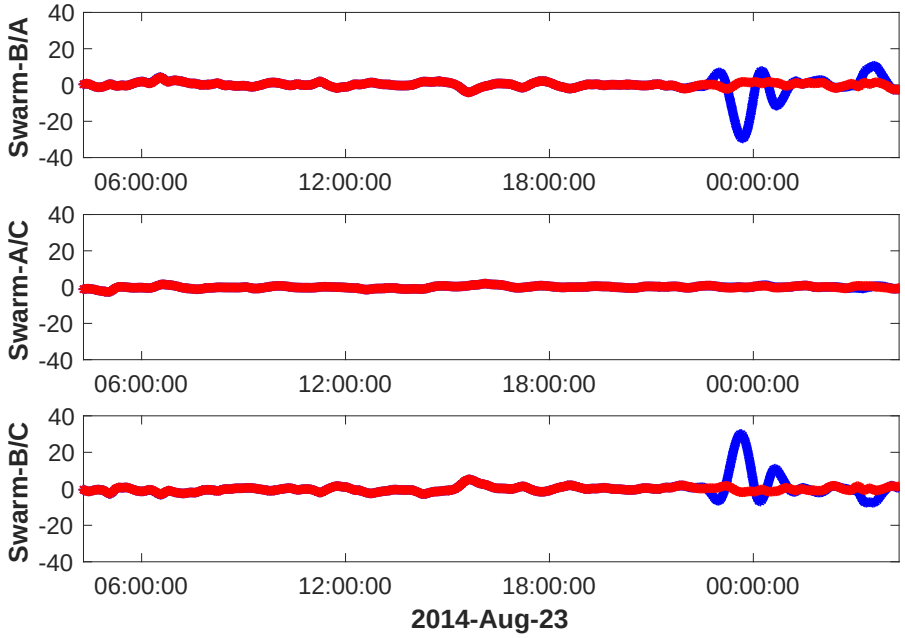


Figure 6: Consistency (unit:cm) between triple-satellite Swarm baseline solutions and baselines derived from the reference GSOC/DLR orbits in the along-track direction, both for including (blue) and excluding (red) the identified G04 outliers (22:50 to 23:50, on 23 August 2014). The consistency is included for the Swarm-B/A (top), Swarm-A/C (middle) and Swarm-B/C (bottom) satellite pairs.

GPS observation outliers are in principle detected automatically by the MODK tool (Section 2.2). It is important to report that for a few GPS satellite tracking passes very large observation residuals were obtained, *i.e.* after the automated outlier detection. This resulted in an unstable IEKF process. Therefore, these observations were excluded manually. To be precise, the following passes were eliminated: GPS Block IIA G04 for Swarm-B from 22:50 to 23:50 on 23 August 2014 (DOY 235) and GPS Block IIR-M G17 for Swarm-A from

23:50 on 04 September (DOY 247) to 00:50 on 05 September 2014. Block IIA GPS satellites are sometimes in eclipse affecting their yaw attitude motion [36]. The outliers for 23 August can be attributed to G04 being in eclipse. The cause for the outliers during the other pass might be the inconsistency of GPS satellite clock corrections spanning midnight. The impact of removing the outlying pass is shown for 23 August 2014 in Figure 6. It can be seen that the impact of the outlying pass reaches a level of 20 centimeters. The eliminated data accounts for less than 0.5% of all GPS available observations. It has to be noted that for PBD the relevant GPS tracking passes are excluded for all three satellites when forming DD combinations.

### *4.2. Dual-satellite PBD*

Three dual-satellite PBD solutions can be obtained for Swarm. For each possible pair of Swarm satellites, selected parameter settings are included in Table 5. An ephemeris comparison is done for each satellite between its MODK dual-satellite PBD solution and external GSOC/DLR solutions (Table 6). As for reduced-dynamic POD, two edges of each orbit often show large inconsistency when comparing with adjacent orbits. These edge effects will be exaggerated by differentiating two GSOC/DLR orbits directly. Therefore two 15 min edges of each MODK or GSOC/DLR orbit are neglected for all baseline comparisons in this research, namely 23-hr baseline comparisons are done instead of 24-hr. An example is shown in Figure 7 for 5 August 2014 (DOY 217), which indicates that the edge effects cause clearly larger inconsistency between two solutions. Therefore these influence will be excluded for the following ephemeris comparisons.

In general the different reduced-dynamic orbit solutions show a good level of consistency: the RMS-about-mean of orbit differences is about 5-7 mm for the radial and cross-track directions. For the along-track direction, this is around 12 mm level, which corresponds to a larger dynamic modeling difference between two institutes. Moreover, the comparison shows mean orbit differences of about 2-5 mm in the radial and cross-track directions. They again indicate

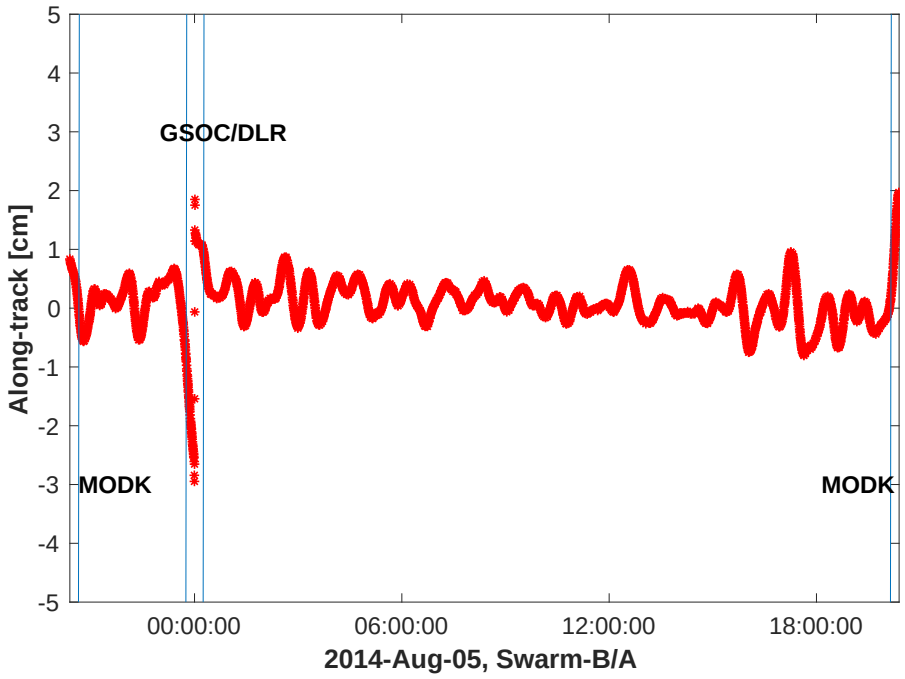


Figure 7: Ephemeris comparison between MODK reduced-dynamic solution and GSOC/DLR single receiver ambiguity fixed reduced-dynamic orbits in along-track direction for the Swarm-B/A baseline (DOY 217, 2014). The excluded edge effects of MODK solution and GSOC/DLR solution are indicated by the legends and blue vertical lines: for the MODK solution, the first and last 15 minutes of an orbit arc are excluded; for the GSOC/DLR solution, the 30 minutes around midnight of an orbit arc are excluded.

the differences between the satellite cannon-ball model used in this research and the panel box-wing macro-model used in [21]. The mean of differences in the radial direction can be attributed to the missing Earth albedo modeling in this research. More sophisticated dynamic modeling of satellite is beneficial for POD and PBD [35, 37], however it goes beyond the scope of this research.

Results of the ephemeris comparisons in terms of baseline are displayed in Table 7. It has to be noted that the GSOC/DLR solutions are provided from midnight to midnight, which differs with the 24-hr arc in this research. The comparisons have been done for both the reduced-dynamic and kinematic MODK baseline solutions. It can be observed that the mean of baseline differences is

Table 6: Ephemeris comparison between different dual-satellite reduced-dynamic MODK baseline solutions and GSOC/DLR single receiver ambiguity fixed reduced-dynamic orbits (mean and RMS-about-mean, 10 orbit arcs).

| Satellite | PBD solution | Radial (mm) | Along-track (mm) | Cross-track (mm) |
|---|---|---|---|---|
| Swarm-A | Swarm-A/C | $4.8 \pm 6.0$ | $-2.8 \pm 12.8$ | $1.4 \pm 7.1$ |
| | Swarm-B/A | $4.9 \pm 6.0$ | $-2.7 \pm 12.4$ | $3.1 \pm 7.1$ |
| Swarm-B | Swarm-B/A | $5.0 \pm 5.3$ | $-0.7 \pm 11.1$ | $3.3 \pm 6.7$ |
| | Swarm-B/C | $5.0 \pm 5.4$ | $-0.4 \pm 11.5$ | $3.2 \pm 7.1$ |
| Swarm-C | Swarm-A/C | $4.7 \pm 5.9$ | $-1.3 \pm 12.8$ | $1.3 \pm 7.2$ |
| | Swarm-B/C | $4.8 \pm 5.7$ | $-0.4 \pm 12.1$ | $2.9 \pm 7.1$ |

very small, typically below 1 mm for the radial and cross-track directions, and below 2.5 mm for the along-track direction. It is clear that common single-satellite orbit errors are canceled to a large extent when forming baselines, *cf.* Table 6. For the reduced-dynamic solutions, a 1-3 mm level consistency is obtained for the Swarm-A/C baseline. This is slightly worse than the level of consistency as reported in [13], in which only a comparison for the Swarm-A/C pair was done and the GSOC/DLR baselines were also DD ambiguity fixed solutions. [13] selected a more quiet ionospheric activity period (January 2016) for comparison. Stronger ionospheric activities bring more challenging issues for precise baseline determination [38]. For the other two reduced-dynamic baselines, larger differences are obtained, which is due to the less favorable geometry between the associated two satellites.

For the kinematic baselines, the consistency between the MODK and the reference GSOC/DLR orbit solutions is worse (Table 7). The consistency level is comparable to the consistency between the MODK reduced-dynamic and kinematic orbit solutions (Table 3). The consistency for Swarm-A/C is better than for Swarm-B/A and Swarm-B/C, which can be attributed to the less favorable

geometry when these satellites are at larger distances. Kinematic solutions will not be computed when less than 5 GPS satellites are in view by two Swarm satellites, therefore the percentage of epochs with available kinematic solutions drops as the distance gets longer for satellite pairs. Another comparison is done between baselines derived from GSOC/DLR kinematic and reduced-dynamic DPOD solutions. It is interesting to observe that for the GSOC/DLR kinematic baseline comparison, a similar level of consistency is obtained for all three baselines, thus including Swarm-A/C. The MODK kinematic baselines display better consistency with the GSOC/DLR DPOD reduced-dynamic reference orbits than the associated GSOC/DLR DPOD kinematic orbits, even for Swarm-B/A and Swarm-B/C formations for which the lengths are varying up to 3500 km. This can be explained by considering that in single-satellite POD, no advantage can be taken of *e.g.* constraining relative dynamics, as are done for Swarm-A/C with the MODK tool. Nevertheless, the GSOC/DLR kinematic solutions for the high-dynamic satellite pairs have around 10% higher availability than the MODK solutions.

### *4.3. Triple-satellite PBD*

When comparing the kinematic and reduced-dynamic baseline consistency obtained by dual-satellite and triple-satellite PBD, respectively, slightly downgraded consistency can be seen for the triple-satellite case in Table 8. Table 9 shows the direct comparison between satellite orbits computed using the triple-satellite PBD mode and the GSOC/DLR single-satellite reference orbit solutions. This in general also corresponds to the results in Table 6. The results indicate that by including a third Swarm satellite leading to high-dynamic baselines does not significantly degrade the baselines solution for the Swarm-A/C pendulum pair.

Table 10 shows the results of comparison between Swarm triple-satellite PBD solutions and baselines derived from the reference GSOC/DLR orbits. When comparing with dual-satellite mode, in general around 2.6% less kinematic solutions are created for Swarm-A/C baseline due to more data editing for three

Table 7: Comparison between different MODK baseline solutions (dual-satellite PBD) and baselines derived from the GSOC/DLR DPOD reduced-dynamic reference orbits (mean and RMS-about-mean, 10 orbit arcs), another comparison is done between the GSOC/DLR DPOD kinematic and reduced-dynamic reference orbits. The percentage of epochs with available kinematic solutions is also shown.

| Solution | Radial (mm) | Along-track (mm) | Cross-track (mm) | Perc. (%) |
|---|---|---|---|---|
| **MODK Reduced-dynamic** | | | | |
| Swarm-A/C | $-0.0 \pm 1.6$ | $2.1 \pm 2.9$ | $-0.1 \pm 1.4$ | 100 |
| Swarm-B/A | $0.7 \pm 4.7$ | $1.6 \pm 6.7$ | $0.2 \pm 3.5$ | 100 |
| Swarm-B/C | $-0.2 \pm 2.9$ | $0.7 \pm 4.3$ | $-0.2 \pm 3.0$ | 100 |
| **MODK Kinematic** | | | | |
| Swarm-A/C | $-0.1 \pm 11.9$ | $2.2 \pm 5.7$ | $-0.1 \pm 3.5$ | 97.7 |
| Swarm-B/A | $-0.2 \pm 22.8$ | $2.0 \pm 12.0$ | $0.4 \pm 6.3$ | 80.2 |
| Swarm-B/C | $0.9 \pm 21.3$ | $0.3 \pm 10.0$ | $-0.4 \pm 5.9$ | 81.3 |
| **DLR DPOD Kinematic** | | | | |
| Swarm-A/C | $0.2 \pm 21.2$ | $0.1 \pm 8.3$ | $-0.1 \pm 6.3$ | 93.7 |
| Swarm-B/A | $-0.1 \pm 25.0$ | $1.0 \pm 11.6$ | $0.0 \pm 7.6$ | 91.7 |
| Swarm-B/C | $0.2 \pm 25.4$ | $-1.0 \pm 11.6$ | $-0.1 \pm 7.6$ | 91.8 |

satellites. Compared to the dual-satellite mode, more single-differenced combinations have to be established and pass the data editing because of the involvement of Swarm-B [15]. It is found that the single-differenced clock offset editing - highly determined by the relative ionospheric changes between two satellites - is the dominant impact factor which discards more than 1% data for each satellite. However for especially Swarm-B/A baseline a slight improvement of 1% is obtained, which can be attributed to more kinematic solutions passing the residual assessment. Dual-satellite PBD mode lacks constraint from the third satellite, therefore more solutions at larger distance will fail to pass this test. The baseline consistency between the MODK kinematic solutions and the

Table 8: Comparison between MODK kinematic and reduced-dynamic baseline solutions, and ambiguity fixing success rate for dual- and triple-satellite PBD (mean of RMS-about-mean statistics of 10 orbit arcs).

| Solution | Radial (mm) | Along-track (mm) | Cross-track (mm) | Amb.fix. (%) |
|---|---|---|---|---|
| | | **Swarm-A/C** | | |
| Dual- | 12.4 | 5.5 | 3.6 | 98.1 |
| Triple- | 13.9 | 6.4 | 4.0 | 98.4 |
| | | **Swarm-B/A** | | |
| Dual- | 22.9 | 9.8 | 5.6 | 97.3 |
| Triple- | 23.4 | 10.0 | 5.8 | 97.3 |
| | | **Swarm-B/C** | | |
| Dual- | 22.6 | 10.4 | 5.7 | 97.5 |
| Triple- | 23.5 | 10.4 | 5.9 | 97.4 |

Table 9: Comparison between the Swarm triple-satellite reduced-dynamic PBD orbits of each satellite and the reference GSOC/DLR reduced-dynamic orbit (mean and RMS-about-mean, 10 orbit arcs).

| Solution | Radial (mm) | Along-track (mm) | Cross-track (mm) |
|---|---|---|---|
| Swarm-A | $4.8 \pm 5.7$ | $-2.7 \pm 12.0$ | $3.8 \pm 7.2$ |
| Swarm-B | $4.9 \pm 5.4$ | $-0.6 \pm 11.6$ | $3.9 \pm 7.1$ |
| Swarm-C | $4.7 \pm 5.7$ | $-0.5 \pm 12.3$ | $3.6 \pm 7.3$ |

reference solutions is similar compared to the result for dual-satellite PBD (Table 7), which corresponds to the results in Tables 8 and 9. Nevertheless, for the triple-satellite PBD, the reduced-dynamic baseline solutions, especially baselines involving Swarm-A, have slightly better agreement with the GSOC/DLR orbits.

For the Swarm-A/C pair an improvement from 1.6/2.9/1.4 to 1.5/2.6/1.4 mm is obtained, for the Swarm-B/A pair 4.7/6.7/3.5 to 3.3/4.7/3.3 mm, and for the Swarm-B/C pair a slight degradation from 2.9/4.3/3.0 to 3.1/4.6/3.1 mm. It will be assessed in Section 4.4 if the absolute orbit solutions are influenced by the triple-satellite PBD.

Table 10: Comparison between different MODK baseline solutions (triple-satellite PBD) and the baselines derived from the reduced-dynamic GSOC/DLR reference orbits (mean and RMS-about-mean, 10 days). The percentage of epochs with available kinematic solutions is also shown.

| Solution | Radial (mm) | Along-track (mm) | Cross-track (mm) | Perc. (%) |
|---|---|---|---|---|
| **MODK Reduced-dynamic** | | | | |
| Swarm-A/C | $-0.1 \pm 1.5$ | $2.2 \pm 2.6$ | $-0.1 \pm 1.4$ | 100 |
| Swarm-B/A | $0.6 \pm 3.3$ | $1.5 \pm 4.7$ | $0.1 \pm 3.3$ | 100 |
| Swarm-B/C | $-0.2 \pm 3.1$ | $0.7 \pm 4.6$ | $-0.2 \pm 3.1$ | 100 |
| **MODK Kinematic** | | | | |
| Swarm-A/C | $-0.0 \pm 13.0$ | $2.2 \pm 6.2$ | $-0.1 \pm 3.8$ | 95.1 |
| Swarm-B/A | $-0.6 \pm 22.2$ | $2.3 \pm 10.0$ | $0.5 \pm 6.2$ | 81.5 |
| Swarm-B/C | $1.1 \pm 22.5$ | $0.1 \pm 10.8$ | $-0.6 \pm 6.3$ | 81.2 |

Figure 8 depicts a one day comparison between two kinematic solutions and the GSOC/DLR-derived reduced-dynamic baseline solution for three satellite pairs. It shows periodic peaks, especially for the Swarm-A/C pair whose baseline length is varying between 30 to 180 km. They fly simultaneously over two poles with the smallest distance. However, they also experience the worst consistency in the polar areas. [39, 13, 14] all report that ionospheric activities clearly deteriorate the POD and PBD solutions above the geomagnetic poles. The ionospheric activity became stronger as the 11-year solar cycle was approaching its peak at the end of 2014.

Figure 9 takes one example and shows the baseline consistency between the

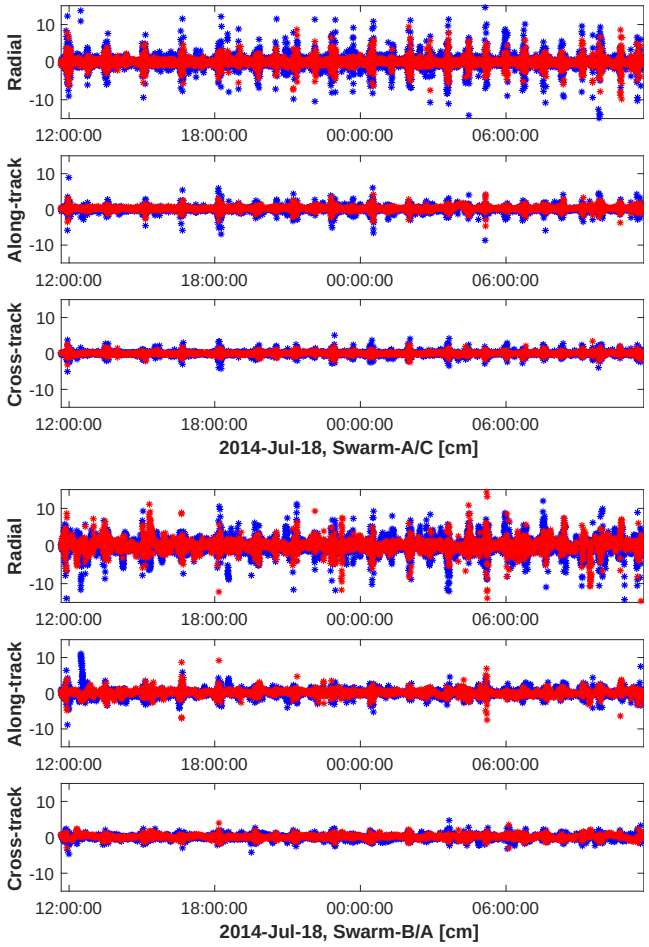


Figure 8: Ephemeris comparison (unit:cm) for the GSOC/DLR(blue) and MODK(red) kinematic baselines for the Swarm-A/C (top), Swarm-B/A(bottom) satellite pairs, the GSOC/DLR DPOD reduced-dynamic baselines are set as reference (DOY 198, 2014). The comparison for Swarm-B/C pair is similar with Swarm-B/A pair.

MODK kinematic and reduced-dynamic solutions as a function of the distance between two associated satellites for a representative day. This consistency is displayed for each individual direction, where the direction is defined by the local-horizontal, local-vertical reference frame (*i.e.* radial, along-track and cross-track direction) of a reference satellite (Swarm-A for Swarm-B/A and Swarm-

A/C formations, and Swarm-B for Swarm-B/C formation). Baseline consistency for the radial direction is the worst, which can be explained by geometry, *i.e.* the largest component of Geometric Dilution Of Precision (GDOP) is in this direction.

Figure 9 also shows that the availability of kinematic solutions drops when the distance between the two associated satellites increases. As shown in Figure 2, the number of simultaneously tracked GPS satellites by two on-board GPS receivers drops when the distance increases. Eventually, there will not be sufficient satellites simultaneously in view to compute a kinematic baseline solution. Apparently the spatial geometry for the more dynamic Swarm-B/A and Swarm-B/C pairs deteriorates more quickly. In general the Swarm-B/A and Swarm-B/C satellite pairs have only 81.5% and 81.2% of epochs with kinematic solutions, respectively, compared to 95.1% for the Swarm-A/C satellite pair (see Table 10). It can be observed in Figure 9 that the consistency between kinematic and reduced-dynamic baselines solutions become slightly worse with increasing distance. The consistency statistics are shown in Table 10, which indicate that 13.0/6.2/3.8 mm is achievable for the Swarm-A/C satellite pair in respectively the radial, along-track and cross-track directions. For the Swarm-B/A satellite pair, a degraded consistency level of 22.2/10.0/6.2 is obtained, similar to the Swarm-B/C satellite pair.

### *4.4. Satellite Laser Ranging*

The availability of SLR observations for the Swarm constellation allows for an independent validation of orbit solutions in the line-of-sight direction between the SLR ground stations and each LEO satellite [40]. An editing threshold of 30 cm is applied, which is more than an order of magnitude above the RMS of fit levels. In addition, observations below a 10° elevation cut-off angle are excluded to eliminate observations with relatively large atmospheric delay correction errors. An SLR retro-reflector correction map from the German Research Center for Geosciences (GFZ) is included [41]. Furthermore, four SLR stations (Arequipa, Hartebeest, Kiev, Simeiz) with large mean offsets are excluded for the

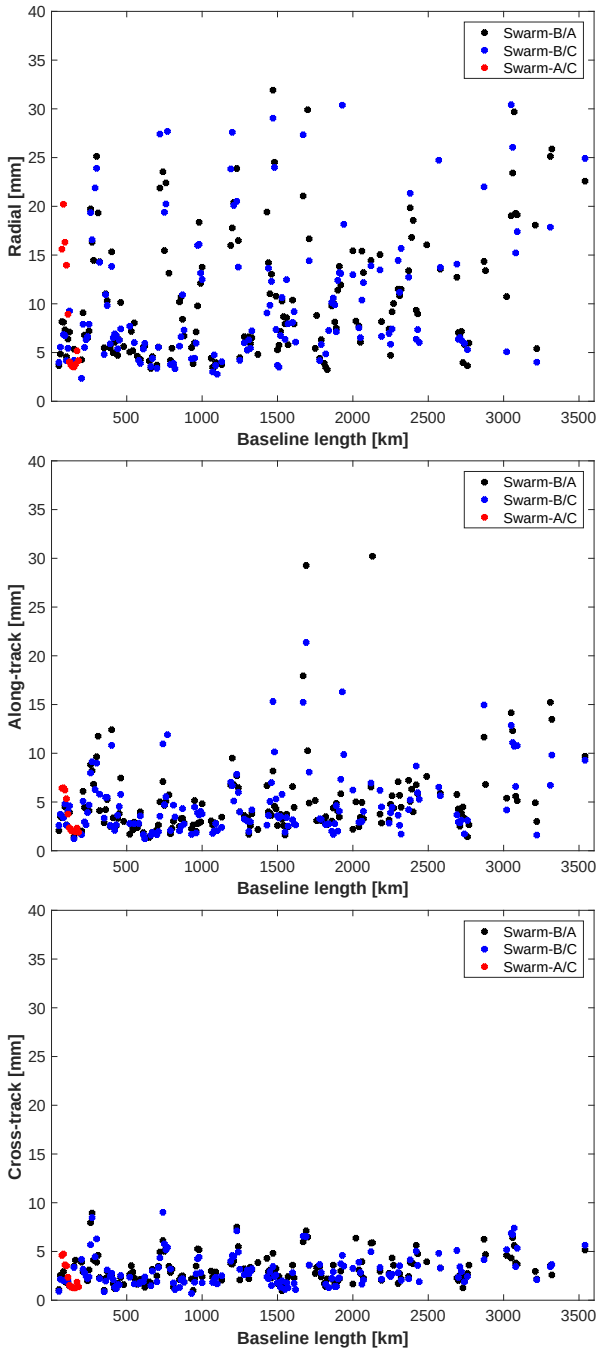


Figure 9: RMS of differences between kinematic and reduced-dynamic solutions as a function of distance (every 10 kms) in the radial (top), along-track (middle) and cross-track (bottom) directions for the three Swarm baselines (DOY 198, 2014).

Swarm SLR validations. Eventually 76.5%(649/848), 80.2%(1385/1726) and 75.3%(510/677) of the SLR observations are used for orbit validation of Swarm-A, -B and -C respectively (Table 11).

It can be observed that for the MODK POD single-satellite orbits the RMS-about-mean of fit of SLR validation is quite close to the reference ESA reduced-dynamic Precise Science Orbits (PSO) [39]. In general, a consistency level (RMS-about-mean) of around 20 mm is achieved for the three Swarm satellites. The best performance is obtained for Swarm-B, which flies at the highest altitude. The best accuracy is found for the GSOC/DLR single-receiver ambiguity fixed solutions. Similar to the analysis in [29, 15], the dual-satellite PBD results in slightly worse SLR consistency levels. Note that for the Swarm-B satellite, the consistency improves for the Swarm-B/C PBD, but not for the Swarm-B/A PBD solution. For the Swarm triple-satellite MODK PBD solution, similar levels are obtained. This indicates good consistency between dual-satellite and triple-satellite modes of MODK.

Table 11: Mean and RMS-about-mean of fit of SLR observations for different reduced-dynamic orbit solutions for the 10 selected orbit arcs.

| Solution | Swarm-A (mm) | Swarm-B (mm) | Swarm-C (mm) |
|---|---|---|---|
| ESA | $1.5 \pm 18.4$ | $-2.8 \pm 14.7$ | $1.9 \pm 21.0$ |
| GSOC/DLR | $1.1 \pm 17.5$ | $1.0 \pm 11.1$ | $1.6 \pm 21.2$ |
| POD | $-1.1 \pm 20.8$ | $-4.0 \pm 14.1$ | $0.8 \pm 21.6$ |
| PBD Swarm-A/C | $-0.7 \pm 21.0$ | NA | $0.7 \pm 22.1$ |
| PBD Swarm-B/A | $-0.8 \pm 19.2$ | $-2.2 \pm 14.3$ | NA |
| PBD Swarm-B/C | NA | $-3.7 \pm 12.7$ | $1.1 \pm 22.3$ |
| PBD Swarm-A/B/C | $-0.9 \pm 19.7$ | $-3.5 \pm 12.9$ | $1.3 \pm 22.2$ |
| No. | 649 | 1385 | 510 |

The Swarm-A/C satellites fly in formation with a baseline below 180 km. Therefore it is possible that an SLR station switches between these two Swarm

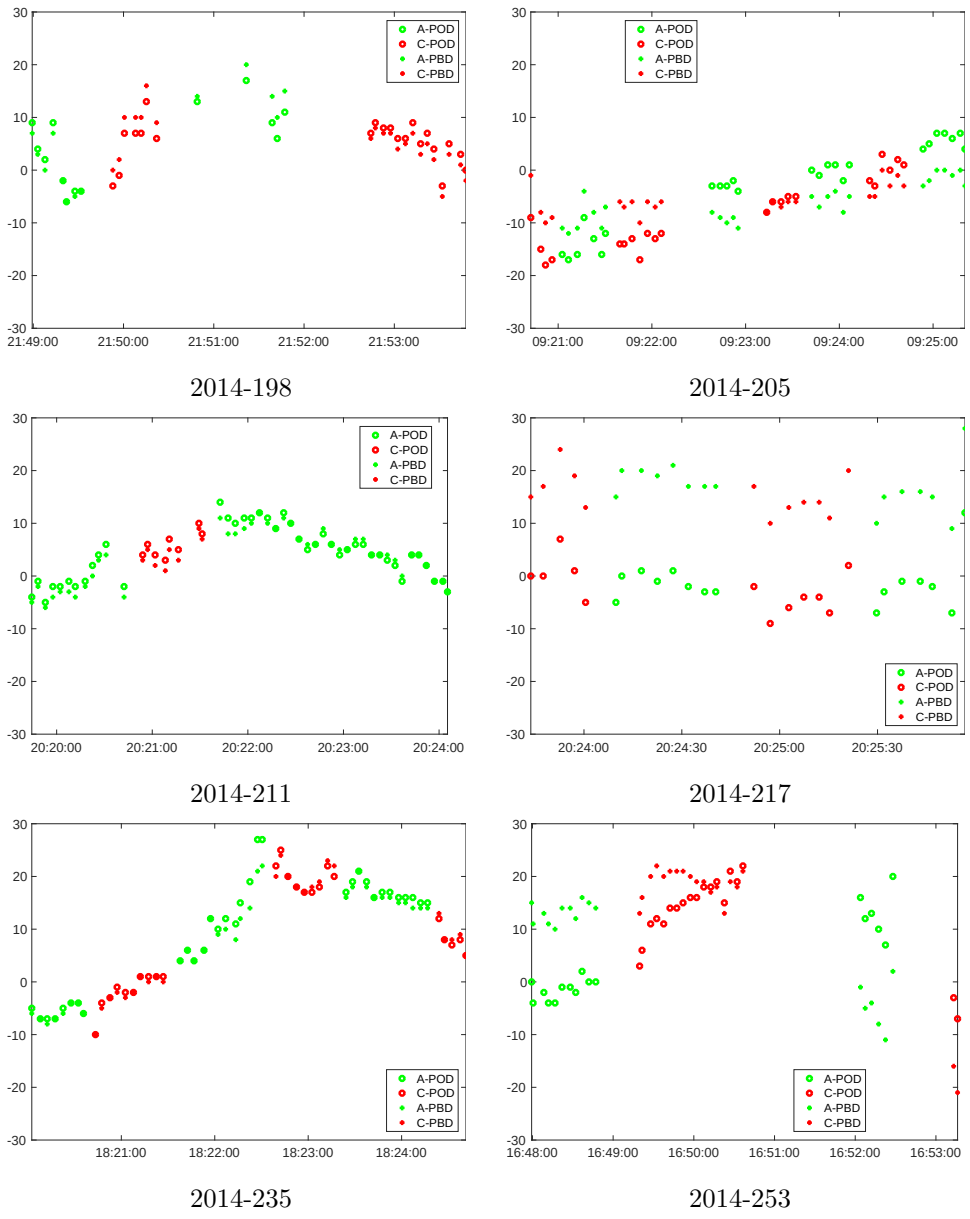


Figure 10: SLR residuals (unit:mm) for the Swarm-A/C single-satellite POD (reference) and dual-satellite PBD orbit solutions by using the well-performing Yarragadee station in Australia. Six tracking passes with more than 27 points are selected. For each pass the DOY in 2014 is indicated.

satellites during one overpass. This offers an additional opportunity to assess the consistency in terms of time series between the two different orbit solutions and the SLR observations. The Yarragadee station in Australia offers the largest number of such overpasses and is therefore selected for this analysis.

When tracking the Swarm-A and C satellites, normally the Yarragadee tracking switches happen 1 to 6 times during the satellite overpass, which typically has a duration of only a few minutes. Figure 10 shows that for DOY 205 in 2014, the SLR residuals are better aligned in time when using the Swarm-A/C dual-satellite PBD solution. For other passes displayed in Figure 10, consistency is at the same level for the PBD solutions as compared to the POD solutions. This result agrees well with results reported in [14] and also similar analysis for the TanDEM-X/TerraSAR-X formation as reported in [42].

Another assessment is done to check the alignment of Swarm-A and -C satellite orbits based on the Swarm-B/A and Swarm-B/C PBD on DOY 205 in 2014. The STDs of all Swarm-A and -C SLR residuals for a tracking pass are computed. A smaller STD means two satellite orbits align closer with the same reference SLR ground station, or in other words, it represents better alignment between two orbits. The STDs of Swarm-A and -C satellite SLR validation residuals for this orbit pass are 7.78, 3.36, 3.12 and 2.48 mm for the single-satellite POD, Swarm-A/C dual-satellite PBD, triple-satellite PBD and the Swarm-A/C baseline based on the Swarm-B/A and Swarm-B/C PBD, respectively. Clearly the alignments for the latter three solutions are very close and are better than the single-satellite POD orbits. The PBD seems to improve the SLR consistency between the Swarm-A and -C satellites for this day. This demonstrates the benefits of relative dynamics constraints between the higher Swarm-B and either of the lower Swarm satellites.

## 5. Conclusions and Recommendations

The three-satellite Swarm constellation has been used as test bed for Swarm dual- and triple-satellite orbit determination, where two of the satellites are fly-

ing in formation and the third one flies in a different orbit. Thus, in addition to relatively slowly varying baselines, also fast changing or high-dynamic baselines are included in the tests. Three different Swarm satellite pairs and thus baselines can be defined: the pendulum baseline (Swarm-A/C) and two high-low baselines (Swarm-B/A and Swarm-B/C), where the high-low baselines can typically be formed during limited periods every 6.1 days. For the latter, the baseline varies from 50 km to 3500 km for orbital arcs with a duration of 24-hr centered around the time of closest approach. Precise Baseline Determination (PBD) for Swarm involving the Swarm-B satellite is challenging because of different levels of dynamic force modeling uncertainty, where it is expected that this is different for Swarm-A and -C. An Iterative Extended Kalman Filter (IEKF) in combination with subset ambiguity fixing is used to compute reduced-dynamic PBD solutions for Swarm. Kinematic PBD solutions are then obtained by using the fixed ambiguities obtained from the reduced-dynamic solutions.

Results show that the GPS receiver RINEX converter and half-cycle to full-cycle ambiguities corrections are very beneficial for PBD. The Swarm reduced-dynamic baseline comparisons with external orbits from the German Space Operations Center (GSOC/DLR) show good baseline consistency at a level of only 1-3 mm for the pendulum Swarm-A/C satellite pair. For the other two pairs, a consistency at a level of 3-5 mm is achieved for different directions. The overall MODK kinematic baseline consistences with its reduced-dynamic baseline are at a level of 13/6/4 mm for Swarm-A/C and a level of 23/11/7 mm for the other two pairs (radial/along-track/cross-track). They are better than the internal consistences between two GSOC/DLR solutions and again indicate the benefits of constraining relative dynamics and fixing Double-Difference (DD) carrier phase ambiguities. However it has to be noted that these consistencies deteriorate when baselines increase.

The research in this paper has shown that triple-satellite PBD including high-dynamic baselines leads to comparable performance in terms of kinematic/reduced-dynamic baseline consistencies and SLR observation fits as dual-satellite PBD. The inclusion of high-dynamic baselines does thus not degrade the quality of the

orbit solutions as was the case in *e.g.* [15]. Compared to single-satellite POD, it was shown that a better Swarm-A/C consistency can be obtained in the time series of SLR observation residuals.

It has also been shown that the consistency between kinematic and reduced-dynamic baseline solutions deteriorates with growing distance, which can be explained to a large extent by a less favorable geometry. A possibility for improvement might be to combine the single-satellite ambiguity fixed method with the PBD ambiguity fixing method used in this paper. This is a nice topic for future research. The single-satellite ambiguity fixed solutions lead to larger kinematic/reduced-dynamic consistency levels at short distance (Table 7), but might suffer less from a deteriorated geometry for longer distances.

## Acknowledgments

The Chinese Scholarship Council (CSC) is gratefully acknowledged for financially supporting part of the work described in this paper. We would like to show our special gratitude to the European Space Agency (ESA) for sharing the Swarm data products. We also very much thank Dr. Oliver Montenbruck from The German Space Operations Center for providing the single-receiver ambiguity fixed orbit solutions and the new version GPS RINEX data. We also acknowledge two anonymous reviewers for reviewing this paper.

## References

[1] C. Sabol, R. Burns, C. A. McLaughlin, Satellite formation flying design and evolution, J. Spacecr. Rockets 38 (2) (2001) 270–278. doi:10.2514/2.3681.

[2] B. D. Tapley, S. Bettadpur, J. C. Ries, P. F. Thompson, M. M. Watkins, GRACE measurements of mass variability in the Earth system, Science 305 (5683) (2004) 503–505.

[3] G. Krieger, A. Moreira, H. Fiedler, I. Hajnsek, M. Werner, M. Younis, M. Zink, TanDEM-X: A satellite formation for high-resolution SAR interferometry, IEEE Trans. Geosci. Remote Sens. 45 (11) (2007) 3317–3341. doi:10.1109/TGRS.2007.900693.

[4] O. Montenbruck, M. Wermuth, R. Kahle, GPS based relative navigation for the TanDEM-X mission-first flight results, Navigation 58 (4) (2011) 293–304. doi:10.1002/j.2161-4296.2011.tb02587.x.

[5] A. Jäggi, C. Dahle, D. Arnold, H. Bock, U. Meyer, G. Beutler, J. van den IJssel, Swarm kinematic orbits and gravity fields from 18 months of GPS data, Adv. Space Res. 57 (1) (2016) 218–233. doi:10.1016/j.asr.2015.10.035.

[6] S.-C. Wu, T. P. Yunck, C. L. Thornton, Reduced-dynamic technique for precise orbit determination of low Earth satellites, J Guid. Control Dyn. 14 (1) (1991) 24–30. doi:10.2514/3.20600.

[7] P. J. Teunissen, An optimality property of the integer least-squares estimator, J. Geod. 73 (11) (1999) 587–593. doi:10.1007/s001900050269.

[8] R. Kroes, O. Montenbruck, W. Bertiger, P. Visser, Precise GRACE baseline determination using GPS, GPS Solut. 9 (1) (2005) 21–31. doi:10.1007/s10291-004-0123-5.

[9] A. Jäggi, U. Hugentobler, H. Bock, G. Beutler, Precise orbit determination for GRACE using undifferenced or doubly differenced GPS data, Adv. Space Res. 39 (10) (2007) 1612–1619.

[10] G. Allende-Alba, O. Montenbruck, Robust and precise baseline determination of distributed spacecraft in LEO, Adv. Space Res. 57 (1) (2016) 46–63. doi:10.1016/j.asr.2015.09.034.

[11] X. Mao, P. Visser, J. van den IJssel, Impact of GPS antenna phase center and code residual variation maps on orbit and baseline determination of

GRACE, Adv. Space Res. 59 (12) (2017) 2987–3002. doi:10.1016/j.asr.2017.03.019.

[12] E. Friis-Christensen, H. Lühr, G. Hulot, Swarm: A constellation to study the Earths magnetic field, Earth Planets Space 58 (4) (2006) 351–358. doi:10.1186/BF03351933.

[13] X. Mao, P. Visser, J. van den IJssel, The impact of GPS receiver modifications and ionospheric activity on Swarm baseline determination, Acta Astronaut. 146 (2018) 399–408. doi:10.1016/j.actaastro.2018.03.009.

[14] G. Allende-Alba, O. Montenbruck, A. Jäggi, D. Arnold, F. Zangerl, Reduced-dynamic and kinematic baseline determination for the Swarm mission, GPS Solut. 21 (3) (2017) 1275–1284. doi:10.1007/s10291-017-0611-z.

[15] P. W. L. van Barneveld, Orbit determination of satellite formations, Ph.D. thesis, Delft University of Technology, ISBN: 9778-94-6191-546-7 (2012).

[16] E. Doornbos, Thermospheric density and wind determination from satellite dynamics, Ph.D. thesis, Delft University of Technology, ISBN: 978-3-642-44264-3 (2012).

[17] O. Montenbruck, T. Van Helleputte, R. Kroes, E. Gill, Reduced dynamic orbit determination using GPS code and carrier measurements, Aerosp. Sci. Technol. 9 (3) (2005) 261–271. doi:10.1016/j.ast.2005.01.003.

[18] O. Montenbruck, R. Kroes, In-flight performance analysis of the CHAMP BlackJack GPS receiver, GPS Solut. 7 (2) (2003) 74–86. doi:10.1007/s10291-003-0055-5.

[19] F. Zangerl, F. Griesauer, M. Sust, O. Montenbruck, S. Buchert, A. Garcia, Swarm GPS precise orbit determination receiver initial in-orbit performance evaluation, Proceedings of the 27th International Technical Meeting of the Satellite Division of the Institute of Navigation (ION-GNSS+-2014), Tampa, Florida (2014) 1459–1468.

[20] O. Montenbruck, S. Hackel, A. Jäggi, Precise orbit determination of the Sentinel-3A altimetry satellite using ambiguity-fixed GPS carrier phase observations, J. Geod. 92 (7) (2017) 711–726. doi:10.1007/s00190-017-1090-2.

[21] O. Montenbruck, S. Hackel, J. van den IJssel, D. Arnold, Reduced dynamic and kinematic precise orbit determination for the Swarm mission from 4 years of GPS tracking, GPS Solut. 22 (79). doi:10.1007/s10291-018-0746-6.

[22] B. D. Tapley, S. Bettadpur, M. Watkins, C. Reigber, The gravity recovery and climate experiment: mission overview and early results, Geophys. Res. Lett. 31 (9) (2004) L0960. doi:10.1029/2004GL019920.

[23] W. Bertiger, S. D. Desai, B. Haines, N. Harvey, A. W. Moore, S. Owen, J. P. Weiss, Single receiver phase ambiguity resolution with GPS data, J. Geod. 84 (5) (2010) 327–337. doi:10.1007/s00190-010-0371-9.

[24] G. Blewitt, Carrier phase ambiguity resolution for the Global Positioning System applied to geodetic baselines up to 2000 km, J. Geophys. Res. Solid Earth 94 (B8) (1989) 10187–10203. doi:10.1029/JB094iB08p10187.

[25] S. Loyer, F. Perosanz, F. Mercier, H. Capdeville, J.-C. Marty, Zero-difference GPS ambiguity resolution at CNES-CLS IGS Analysis Center, J. Geod. 86 (11) (2012) 991. doi:10.1007/s00190-012-0559-2.

[26] J. J. Degnan, Millimeter accuracy satellite laser ranging: a review, Contributions of space geodesy to geodynamics: technology (1993) 133–162doi:10.1029/GD025p0133.

[27] N. Olsen, R. Haagmans, T. J. Sabaka, A. Kuvshinov, S. Maus, M. E. Purucker, M. Rother, V. Lesur, M. Mandea, The Swarm End-to-End mission simulator study: A demonstration of separating the various contributions to Earth's magnetic field using synthetic data, Earth Planets Space 58 (4) (2006) 359–370. doi:10.1186/BF03351934.

[28] R. Dach, S. Schaer, D. Arnold, L. Prange, D. Sidorov, P. Stebler, A. Villiger, A. Jäggi, Code final product series for the IGS, Tech. rep., Astronomical Institute, University of Bern (2018). doi:10.7892/boris.75876.3.

[29] R. Kroes, Precise relative positioning of formation flying spacecraft using GPS, Ph.D. thesis, Delft University of Technology, ISBN: 90-8559-150-3, (2006).

[30] J. van den IJssel, B. Forte, O. Montenbruck, Impact of Swarm GPS receiver updates on POD performance, Earth Planets Space 68 (1) (2016) 1–17. doi:10.1186/s40623-016-0459-4.

[31] T. P. Yunck, Orbit determination, Prog. Astronaut. Aeronaut. 164 (1996) 559–592. doi:10.2514/5.9781600866395.0559.0592.

[32] M. Wermuth, O. Montenbruck, T. Van Helleputte, GPS high precision orbit determination software tools (GHOST), in: Proceedings of 4th International Conference on Astrodynamics Tools and Techniques, Madrid, ESA WPP-308, 2010, pp. 3–6.

[33] A. Jäggi, R. Dach, O. Montenbruck, U. Hugentobler, H. Bock, G. Beutler, Phase center modeling for LEO GPS receiver antennas and its impact on precise orbit determination, J. Geod. 83 (12) (2009) 1145–1162. doi:10.1007/s00190-009-0333-2.

[34] S. Verhagen, The GNSS integer ambiguities: estimation and validation, Ph.D. thesis, Delft University of Technology, ISBN: 90-804-1474-3 (2005).

[35] S. Hackel, O. Montenbruck, P. Steigenberger, U. Balss, C. Gisinger, M. Eineder, Model improvements and validation of TerraSAR-X precise orbit determination, J. Geod. 91 (5) (2017) 547–562. doi:10.1007/s00190-016-0982-x.

[36] O. Montenbruck, R. Schmid, F. Mercier, P. Steigenberger, C. Noll, R. Fatkulin, S. Kogure, A. S. Ganeshan, GNSS satellite geometry and

attitude models, Adv. Space Res. 56 (6) (2015) 1015–1029. doi:10.1016/j.asr.2015.06.019.

[37] A. Calabia, S. Jin, Assessment of conservative force models from GRACE accelerometers and precise orbit determination, Aerosp. Sci. Technol. 49 (2016) 80–87. doi:10.1016/j.ast.2015.11.034.

[38] U. Tancredi, G. Allende-Alba, A. Renga, O. Montenbruck, M. Grassi, Relative positioning of spacecraft in intense ionospheric conditions by GPS, Aerosp. Sci. Technol. 43 (2015) 191–198. doi:10.1016/j.ast.2015.02.020.

[39] J. van den IJssel, J. Encarnação, E. Doornbos, P. Visser, Precise science orbits for the Swarm satellite constellation, Adv. Space Res. 56 (6) (2015) 1042–1055. doi:10.1016/j.asr.2015.06.002.

[40] M. R. Pearlman, J. J. Degnan, J. Bosworth, The international laser ranging service, Adv. Space Res. 30 (2) (2002) 135–143. doi:10.1016/S0273-1177(02)00277-6.

[41] R. Neubert, L. Grunwaldt, J. Neubert, The retro-reflector for the CHAMP satellite: final design and realization, in: Proceedings of the 11th International Workshop on Laser Ranging, 1998, pp. 260–270.
URL http://ilrs.gsfc.nasa.gov/docs/rra_champ.pdf,LastAccess:05/Dec/2017.

[42] D. Arnold, O. Montenbruck, S. Hackel, K. Sośnica, Satellite laser ranging to low Earth orbiters: orbit and network validation, J. Geod. (2018) 1–20doi:10.1007/s00190-018-1140-4.